Impact of the joint detection-estimation approach on random effects group studies in fMRI

Solveig Badillo, Thomas Vincent, Philippe Ciuciu

IMPACT OF THE JOINT DETECTION-ESTIMATION APPROACH ON RANDOM EFFECTS GROUP STUDIES IN FMRI

Solveig Badillo, Thomas Vincent and Philippe Ciuciu

CEA, Neurospin, Bât. 145 - Point Courrier 156
F-91191 Gif-sur-Yvette, cedex France
Email: firstname.lastname@cea.fr

ABSTRACT

Inter-subject analysis of functional Magnetic Resonance Imaging (fMRI) data relies on single intra-subject studies, which are usually conducted using a massively univariate approach. In this paper, we investigate the impact of an improved intra-subject analysis on group studies. basically the *joint detection-estimation* (JDE) framework [**?**, 1, 2] where an explicit characterization of the Hemodynamic Response Function (HRF) is performed at a regional scale and a stimulus-specific adaptive spatial correlation model enables the detection of activation clusters at voxel level. For the group statistics, we conducted several Random effect analyses (RFX) which relied either on the General Linear Model (GLM), or on the JDE analyses, or even on an intermediate approach named Spatially Adaptive GLM (SAGLM). Our comparative study perfomed during a fast-event related paradigm involves 18 subjects and illustrates the region-specific differences between the GLM, SAGLM and JDE analyses in terms of statistical sensitivity. On different contrasts of interest, spatial regularization is shown to have a beneficial impact on the statistical sensitivity. Also, by studying the spatial variability of the HRF, we demonstrate that the JDE framework provides more robust detection performance in cognitive regions due to the higher hemodynamic variability in these areas.

Index Terms— fMRI, group analysis, RFX, GLM, joint detection-estimation, hemodynamics, Bayesian inference.

1. INTRODUCTION

In fMRI studies, two strategies are available to improve the quality of the data (such as reducing distorsion artifacts and/or improving spatial and temporal resolution). The first approach *(i)* consists in developing advanced estimation techniques while the second one *(ii)* rests on improved acquisition setups at higher static magnetic fields or using parallel imaging. The analysis methods developed in *(i)* are both robust against noise and able to adapt properly to the underlying physiology, by modeling the spatio-temporal fluctuations of the observed BOLD (Blood Oxygen Level Dependent) signal. In this respect, a Bayesian detection-estimation approach has been proposed in [**?**, 2]. This method jointly detects which parts of the brain are involved in a given task or stimulus and estimates the underlying dynamics of activations. Further extended in [1], Adaptive Spatial Mixture Models (ASMM) have been introduced to model spatial correlation of fMRI data instead of uniformly smoothing them.

A previous work [3] has assessed the improvement provided by a *supervised* JDE approach where the maount of spatial correlation was set empirically compared to the classical GLM-based framework using SPM5[1]. The present paper generalizes this previous contribution [3] in the following directions: a) it studies the impact of automatic and spatially adaptive regularization and b) it enables the comparison of *spatially unsupervised* JDE framework [1] with both the GLM-based inference and and the SAGLM approach or the *constrained* JDE version in which the HRF is fixed to its canonical shape. Here, we show results for a large dataset acquired on a 32-channel head coil at a high (2x2 mm^2) in-plane resolution. However, our global study investigated both issues *(i)* and *(ii)* by comparing the impact of using different spatial resolutions, acceleration factors and reconstruction algorithms in a parallel imaging context on group statistics.

This paper is structured as follows. For the sake of self-consistency, the classical fMRI analysis framework is summarized in Section 2. The JDE approach is presented in Section **??**. It relies on a prior parcellation of fMRI data, which derives from a clustering procedure that preserves connectivity and functional homogeneity. Then, at the parcel level the JDE framework allows us to specify and estimate a specific BOLD model. Section **??** is devoted to group studies in fMRI where the principles of random effect analysis are reminded. In Section **??**, results obtained at the group level using different subject-level inferences are compared on two salient contrasts of interest of a quick fMRI mapping experiment. A special attention is paid to the HRF variability in the motor and parietal regions. Conclusions are drawn in Section **??**.

[1] `http://www.fil.ion.ucl.ac.uk/spm`

2. CLASSICAL WITHIN-SUBJECT ANALYSIS IN fMRI

2.1. Standard GLM-based approach

GLM-based methods correspond to hypothesis-driven approaches that postulate a canonical shape for the HRF $\boldsymbol{h}_c$ and enable voxelwise inference. In its simplest form, the model of the BOLD response is spatially invariant and remains constant across the brain. Hence, each regressor in the *design* matrix $\boldsymbol{X}$ is built as the convolution of $\boldsymbol{h}_c$ with the stimulation signal $\boldsymbol{x}^m$ associated with the m^{th} stimulus type. The GLM therefore reads:

$$[\boldsymbol{y}_1, \ldots, \boldsymbol{y}_J] = \boldsymbol{X}\,[\boldsymbol{\beta}_1, \ldots, \boldsymbol{\beta}_J] + [\boldsymbol{b}_1, \ldots, \boldsymbol{b}_J] \quad (1)$$

where $\boldsymbol{y}_j$ is the fMRI time series measured in voxel V_j at times $(t_n)_{n=1:N}$ and $\boldsymbol{\beta}_j \in \mathbb{R}^M$ defines the vector of BOLD effects in V_j for all stimulus type $m = 1 : M$. Noise $\boldsymbol{b}_j$ is usually modelled as a first-order autoregressive (*i.e.,* AR(1)) process in order to account for the spatially-varying temporal correlation of fMRI data [4]: $b_{j,t_n} = \rho_j\, b_{j,t_{n-1}} + \varepsilon_{j,t_n}$, $\forall j,\, t$, with $\boldsymbol{\varepsilon}_j \sim \mathcal{N}(\boldsymbol{0}_N, \sigma^2_{\varepsilon_j} \boldsymbol{I}_N)$, where $\boldsymbol{0}_N$ is a null vector of length N, and $\boldsymbol{I}_N$ stands for the identity matrix of size N. Then, the BOLD magnitudes estimates $\widehat{\boldsymbol{\beta}}_j$ are computed in the maximum likelihood sense as follows: $\widehat{\boldsymbol{\beta}}_j = \arg\min_{\boldsymbol{\beta}\in\mathbb{R}^M} \|\boldsymbol{y}_j - \boldsymbol{X}\boldsymbol{\beta}_j\|^2_{\widehat{\sigma}^{-2}_{\varepsilon_j}\widehat{\boldsymbol{\Lambda}}_j}$, where $\widehat{\sigma}^{-2}_{\varepsilon_j}\widehat{\boldsymbol{\Lambda}}_j$ defines the inverse of the estimated autocorrelation matrix of $\boldsymbol{b}_j$; see [5] for details about the identification of the noise. Later, extensions that incorporate prior information on the BOLD effects $(\boldsymbol{\beta}_j)_{j=1:J}$ have been developed in the Bayesian framework [**?**, 6]. In such cases, vectors $(\widehat{\boldsymbol{\beta}}_j)_{j=1:J}$ are computed using more computationally demanding strategies. However, all these contributions consider a unique and global model HRF model while intra-individual differences in its characteristics have been exhibited between cortical areas [7].

2.2. Flexible GLM models

Although smaller than inter-individual fluctuations, the intra-subject regional variability of the HRF is large enough to be treated with care. GLM can actually be refined to account for variations of the canonical HRF $\boldsymbol{h}_c$ at the voxel level through additional regressors: $\boldsymbol{h}_c$ can be supplemented with its first and second derivatives $([\boldsymbol{h}_c \,|\, \boldsymbol{h}'_c \,|\, \boldsymbol{h}''_c])$ to model eg. differences in time-to-peak. Although powerful and elegant, flexibility is achievable at the expense of fewer effective degrees of freedom and decreased sensitivity in any subsequent statistical test. In this case, the BOLD effect is modelled using several regressors ($\boldsymbol{\beta}^m_j \in \mathbb{R}^P$) and the Student-t statistic can no longer be used to infer on differences $\boldsymbol{\beta}^m_j - \boldsymbol{\beta}^n_j$ between the m^{th} and n^{th} stimulus types. Rather, an *unsigned* Fisher statistic has to be computed, making direct interpretation of activation maps more difficult.

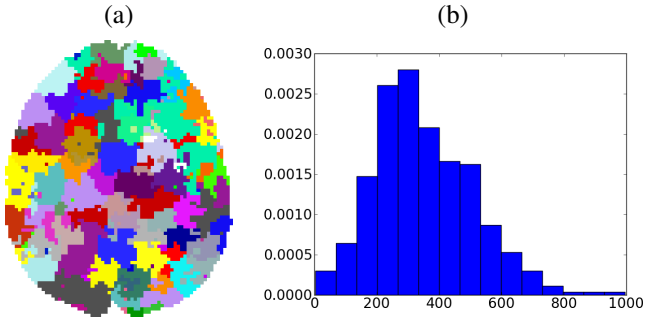

Fig. 1. (a) Axial view of a color-coded multi-subject parcellation. (b): normalized histogram of parcel sizes for the same parcellation.

3. BEYOND THE GLM TO WITHIN-SUBJECT ANALYSIS IN fMRI

3.1. Multi-subject parcellation

Here, we claim the necessity of a spatially varying HRF model to keep a *single* regressor per condition, and thus enable the direct statistical comparison $(\widehat{\beta}^m_j - \widehat{\beta}^n_j)$. The JDE framework proposed in [**?**, 1, 2] enables the introduction of a spatially adaptive GLM, where a local estimation of $\boldsymbol{h}$ is performed. To conduct the analysis efficiently, HRF estimation is performed at a regional coarser scale than the voxel level. To define this scale, the functional brain mask is divided in Γ functionally homogeneous *parcels* using a parcellation technique proposed in [8]. This algorithm relies on the minimization of a compound criterion reflecting both the spatial and functional structures and hence the topology of the dataset. The spatial similarity measure favours the closeness in the Talairach coordinates system. The functional part of this criterion is computed on parameters that characterize the functional properties of the voxels (eg, fMRI time series).

The number of parcels Γ is set by hand. The larger the number of parcels, the stronger the degree of within-parcel homogeneity but potentially the lower the signal-to-noise ratio (SNR). To objectively choose an adequate number of parcels, theoretic information criteria have been investigated in [**?**]: converging evidence for $\Gamma \approx 500$ has been shown for a whole brain analysis leading to typical parcel sizes around a few hundreds voxels. Fig. **??** illustrates the group-level parcellation and the corresponding histogram of parcel sizes.

3.2. Parcel-based modeling of the BOLD signal

Here, we use the parcel-based model of the BOLD signal introduced in [1, 2]. Let $\mathcal{P}_\gamma = (V_j)_{j=1:J}$ be the current parcel. As shown in Fig. 1, this means that the HRF shape $\boldsymbol{h}_\gamma$ is constant within a parcel but that the magnitude of activation β^m_j may vary in space and across stimulus types:

$$\boldsymbol{y}_j = \sum_{m=1}^{M} \beta^m_j \boldsymbol{X}^m \boldsymbol{h}_\gamma + \boldsymbol{P}\boldsymbol{\ell}_j + \boldsymbol{b}_j, \quad \forall\, j,\, V_j \in \mathcal{P}_\gamma. \quad (2)$$

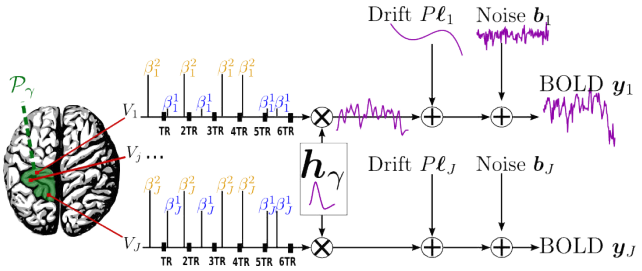

Fig. 2. Regional model of the BOLD signal in the JDE framework. The neural response levels a_j^m match with the BOLD effects β_j^m.

$\boldsymbol{X}^m$ denotes the $N \times (D+1)$ binary matrix that codes the onsets of the m^{th} stimulus. Vector $\boldsymbol{h}_\gamma \in \mathbb{R}^{D+1}$ represents the unknown HRF shape in $\mathcal{P}_\gamma$. The term $\boldsymbol{P}\boldsymbol{\ell}_j$ models a low-frequency trend to account for physiological artifacts and noise $\boldsymbol{b}_j \sim \mathcal{N}(\boldsymbol{0}_N, \sigma_{\varepsilon_j}^2 \boldsymbol{\Lambda}_j^{-1})$ stands for the above mentioned AR(1) process.

3.3. Bayesian JDE inference

The HRF shape $\boldsymbol{h}_\gamma$ and the associated BOLD effects $(\boldsymbol{\beta}_j)_{j=1:J}$ are jointly estimated in $\mathcal{P}_\gamma$. Since no parametric model is considered for $\boldsymbol{h}_\gamma$, a smoothness constraint on the second order derivative is introduced to regularize its estimation; see [2] for details. On the other hand, our approach also aims at *detecting* which voxels in $\mathcal{P}_\gamma$ elicit activations in response to stimulation. To this end, prior mixture models are introduced on $(\boldsymbol{\beta}^m)_{m=1:M}$ to segregate activating and non-activating voxels in a stimulus-specific manner i.e., for each m. In [1], it has been shown that ASMM allow us to recover clusters of activation instead of isolated spots using hidden Markov models on voxel states. The level of spatial correlation in these models is automatically tuned from the data and may vary accross brain regions and between conditions since both the contrast-to-noise ratio the spatial activation pattern fluctuate accross stimulus types.

As our approach stands in the Bayesian framework, other priors are formulated upon every other sought object in Eq. (2); see [1] for details. Finally, inference is based upon the full posterior distribution $p(\boldsymbol{h}, (\boldsymbol{\beta}_j), (\boldsymbol{\ell}_j), \boldsymbol{\Theta} \,|\, \mathbb{y})$, which is sampled using a hybrid Metropolis-Gibbs sampling scheme [1]. Posterior mean (PM) estimates are therefore computed from these samples according to: $\widehat{x}^{\text{PM}} = \sum_{k=L_0}^{L_1} x^{(k)}/L, \quad \forall\, x \in \{\boldsymbol{h}, (\boldsymbol{\beta}_j), \boldsymbol{\Theta}\}$ where $L = L_1 - L_0 + 1$ and L_0 stands for the length of the burn-in period. Note that this estimation process has to be repeated over each parcel of each subject's brain. Since the fMRI data are considered spatially independent across parcels, parallel implementation enables fast computation: whole brain analysis is achievable in about 60 mn for $N = 128$ and $\Gamma = 500$. Compared to [3] which resorted to supervised estimation, the use of ASMM does not significantly increase the computation load since a specific min-max procedure has been developed to approximate parcel-dependent partition functions of MRFs [1]. In this paper, we also investigate the use of ASMM combined with the GLM framework by setting the HRF shape to the canonical form in the JDE formalism. This approach is referenced SAGLM in what follows.

4. CLASSICAL PARAMETRIC POPULATION-BASED INFERENCE

Assume that S subjects are selected randomly in a population of interest and involved in the same fMRI experiment. As shown in previous sections, the two types of within-subject analyses produce BOLD effect estimates $\widehat{\boldsymbol{\beta}}_{j,s}$, in one particular voxel V_j of the standardized space (usually, the MNI/Talairach space) and for each subject s. Comparison between experimental conditions is usually addressed through contrast definition. Here, we restrict ourselves to scalar contrasts. Hence, we focus on signed differences $\widehat{d}_{j,s}^{m-n} = \widehat{\beta}_{j,s}^m - \widehat{\beta}_{j,s}^n$ of the BOLD effect relative to the m^{th} and n^{th} stimulus types. For the sake of notational simplicity, we drop subscript j and superscript $m-n$.

While the estimated difference $\widehat{d}_s$ generally differs from the true but unobserved effect d_s, assume for now perfect intra-subject estimation so that $\widehat{d}_s = d_s$ for $s = 1:S$. We thus are given a sample $(d_1, , \ldots, d_S)$ drawn from an unknown probability density function $f(d)$ that describes the distribution of the effects in the population. Here, we are concerned with inferences about a location parameter (mean, median, mode, ...). Assume for instance we wish to test the null hypothesis that the population mean is negative: $H_0 : \mu_{\text{G}} = \int d\, f(d)\, dd \leq 0$ where $_{\text{G}}$ stands for the group. To that end, we may use the classical one-sample t test. We start with computing the t statistic:

$$t = \frac{\hat{\mu}_{\text{G}}}{\hat{\sigma}_{\text{G}}/\sqrt{S}}, \text{ with } \hat{\mu}_{\text{G}} = \frac{\sum_s d_s}{S}, \; \hat{\sigma}_{\text{G}}^2 = \frac{\sum_s (d_s - \hat{\mu}_{\text{G}})^2}{S-1}.$$

Next, we reject H_0, hence accept the alternative H_1: $\mu_{\text{G}} > 0$, if the probability under H_0 of reaching the observed t value is lower than a given false positive rate. Under the assumption that $f(d)$ is gaussian, this probability is well-known to be obtained from the Student distribution with

5. EXPERIMENTAL RESULTS

5.1. Experimental protocol

fMRI data were recorded at 3 T (Siemens Trio) using a gradient-echo EPI sequence (TE=30ms/TR=2400ms/slice thickness=3mm/transversal orientation/FOV=192mm^2) during a cognitive localizer experiment. The paradigm was a fast event-related design comprising sixty auditory, visual and motor stimuli, defined in ten experimental conditions (auditory and visual sentences, auditory and visual calculations,

left/right auditory and visual clicks, horizontal and vertical checkerboards). For the considered dataset, the acquisition consisted of a single session of $N = 128$ scans lasting $TR = 2.4$ s each, yielding 3-D volumes with an anisotropic resolution of $2 \times 2 \times 3\text{mm}^3$. A 32 channel volume coil was used to enable parallel imaging. The mSENSE parallel imaging reconstruction algorithm was applied with an acceleration factor $R = 2$ for all the 18 subjects[2].

5.2. Random effect (RFX) analyses

To enforce the coherence of our group level comparison with actual pipelines for fMRI data processing (SPM, FSL, BrainVISA-fMRI toolbox), the fMRI images that enter in GLM-based analysis were spatially filtered using isotropic Gaussian smoothing at FWHM=3mm. However, in the JDE formalism, we still consider *unsmoothed* but normalized fMRI data. The contrast images used for the two group analyses (based on intra-subjects analyses with SPM or JDE frameworks) remained also *unsmoothed*.

Figs. **??** and **??** provide us with the group level Student-t maps for the three estimation procedures and two contratsts of interest. Fig. **??** focus on the **Lc. – Rc.** contrast that highlights brain regions responding more to the left click than to the right click whatever the modality (auditory or visual). It is shown that the classical GLM-based, JDE-based and SAGLM-based inferences qualitatively yield almost the same results: a contralateral cluster in the motor cortex is found by all inference schemes. Due to spatial smoothing, GLM-based inference exhibits a larger cluster than alternative approaches but retrieves a lower voxel-level maximum T-value value than the SAGLM-based inference as shown in Table 1. Also, for this motor contrast, we observe that the JDE framework provides the less sensitive results because the estimated HRF shape closely matches the canonical one in motor areas.

Fig. **??** presents the same comparison for the more cognitive **Computation – Sentences (C. – S.)** contrast that elicits evoked brain activity in the fronto-parietal network. Here, the SAGLM-based inference provides larger activation cluster in the parietal and frontal lobes as expected [**?**]. This indicates the strong impact of spatially adaptive regularization. However, the JDE framework gives the highest T-max peak value demonstrating that a better HRF modeling enhances the fit to fMRI data in higher cognitive regions. For this **C. – S.** contrast, the GLM-based inference appears to be the less sensitive both at the voxel and cluster levels: see Table 1 for details. Besides, the GLM and SAGLM-based analyses found one cluster in the right prefrontal gyrus that was not recovered in [**?**], indicating the presence of false positives in this region.

These results are explained by the hemodynamic variability between the motor and parietal regions: HRF estimates

[2]One k-space line out of two was sampled along the phase encoding direction.

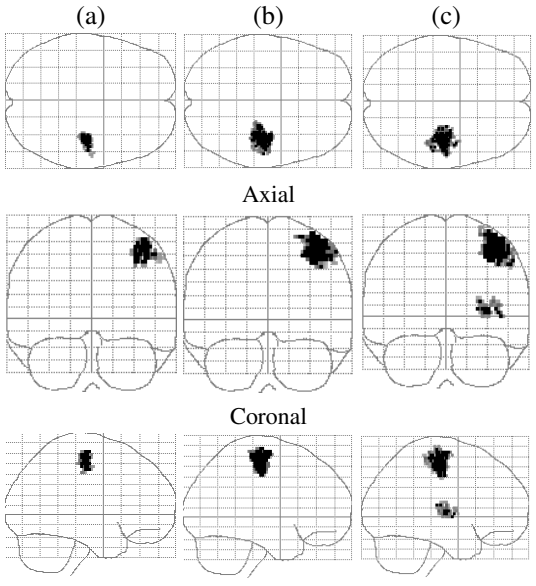

Fig. 3. Maximum Intensity Projection (MIP) of the RFX student-t maps for the **Lc. – Rc.** contrast (thresholded at $P \leq 0.001$ and $K = 100$ for voxel-level and cluster-extent inferences, respectively). **Neurological** convention: left is left. Columns **(a)-(b)-(c)**: results derived using the JDE, SPM, SAGLM analyses at the subject level, respectively.

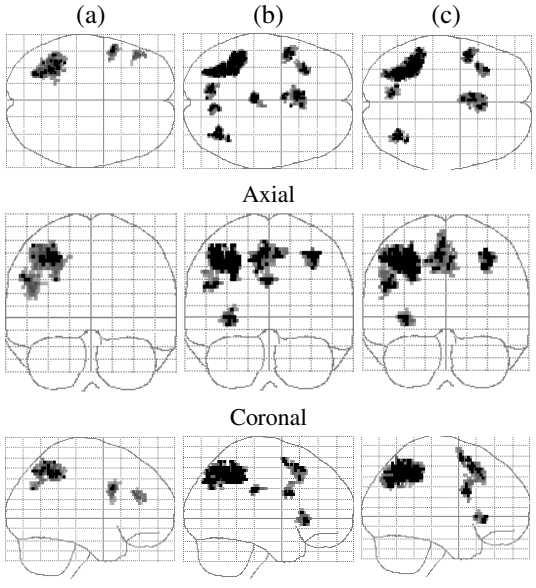

Fig. 4. MIP of the RFX student-t maps for the **C. – S.** contrast. Same conventions as in Fig. **??**

.

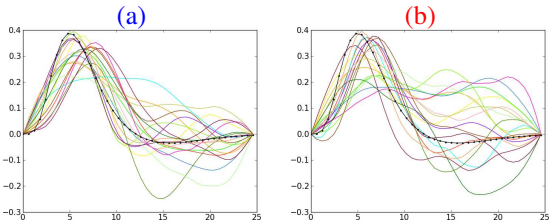

Fig. 5. HRF estimates at the maximum intensity peak for all subjects. **(a)**-**(b)** correspond to the **Lc. – Rc.** and **C. – S.** contrasts, respectively. Canonical HRF in black dotted line.

in the motor region have a shape closer to the canonical form (Fig. 4(a)) in contrast to their counterpart in the parietal region (Fig. 4(b)). Hence, there is a loss in statistical sensitivity when estimating the HRF shape in motor regions as reported on group studies in Fig. **??**. In more cognitive regions, HRF estimation is beneficial since group-level results are more sensitive than those obtained considering a canonical HRF.

Table 1. Suprathreshold clusters summary for the t-statistic.

		Cluster size (voxels)	Voxel level T max	Peak coords. x	y	z
C. – S.	JDE	514	**10.77**	−32	−54	45
	SPM	617	8.7	−28	−66	48
	SAGLM	**780**	10.59	−30	−56	45
Lc. – Rc.	JDE	169	6.76	44	−16	48
	SPM	**454**	10.12	36	−22	54
	SAGLM	390	**12.21**	38	−22	57

6. CONCLUSION

In this paper, we extended previous results (see [3]) and showed that the type of intra-subject analysis impact group-level statistical analysis: Either the JDE formalism or the SAGLM framework provides more reliable RFX analysis results. In the parietal region, the JDE framework reported higher statistical peak values than SAGLM and GLM-based counterparts due to the high variability of the HRF in this area. In contrast, the SAGLM approach achieves the best compromise in the motor region because of spatially adaptive regularization. This seems to be due to a HRF shape closer to the canonical filter in this region. Future work will be devoted to a more extensive analysis of the between-regions hemodynamic variability.

7. REFERENCES

[1] T. Vincent, L. Risser, and P. Ciuciu, "Spatially adaptive mixture modeling for analysis of within-subject fMRI time series," *IEEE Trans. Med. Imag.*, vol. 29, no. 4, pp. 1059–1074, Apr. 2010.

[2] S. Makni, J. Idier, T. Vincent, B. Thirion, G. Dehaene-Lambertz, and P. Ciuciu, "A fully Bayesian approach to the parcel-based detection-estimation of brain activity in fMRI," *Neuroimage*, vol. 41, no. 3, pp. 941–969, July 2008.

[3] P. Ciuciu, T. Vincent, A.-L. Fouque, and A. Roche, "Improved fMRI group studies based on spatially varying non-parametric BOLD signal modeling," in *5th Proc. IEEE ISBI*, Paris, France, May 2008, pp. 1263–1266.

[4] K.J. Worsley, C.H. Liao, J. Aston, V. Petre, G.H. Duncan, F. Morales, and A.C. Evans, "A general statistical analysis for fMRI data," *Neuroimage*, vol. 15, no. 1, pp. 1–15, Jan. 2002.

[5] W. D. Penny, S. Kiebel, and K. J. Friston, "Variational Bayesian inference for fMRI time series," *Neuroimage*, vol. 19, no. 3, pp. 727–741, 2003.

[6] M. Woolrich, M. Jenkinson, J. Brady, and S. Smith, "Fully Bayesian spatio-temporal modelling of fMRI data," *IEEE Trans. Med. Imag.*, vol. 23, no. 2, pp. 213–231, Feb. 2004.

[7] Daniel A. Handwerker, John M. Ollinger, , and Mark D'Esposito, "Variation of BOLD hemodynamic responses across subjects and brain regions and their effects on statistical analyses," *Neuroimage*, vol. 21, pp. 1639–1651, 2004.

[8] B. Thirion, G. Flandin, P. Pinel, A. Roche, P. Ciuciu, and J.-B. Poline, "Dealing with the shortcomings of spatial normalization: Multi-subject parcellation of fMRI datasets," *Hum. Brain Mapp.*, vol. 27, no. 8, pp. 678–693, Aug. 2006.

[9] Phillip Good, *Permutation, Parametric, and Bootstrap Tests of Hypotheses*, Springer, 3rd edition edition, 2005.